Journal of Biomechanics 43 (2010) 1870–1875

Contents lists available at ScienceDirect

Journal of Biomechanics

journal homepage: www.elsevier.com/locate/jbiomech
www.JBiomech.com

Anomalous fiber realignment during tensile loading of the rat facet capsular ligament identifies mechanically induced damage and physiological dysfunction

Kyle P. Quinn, Joel A. Bauman, Nathan D. Crosby, Beth A. Winkelstein*

Spine Pain Research Laboratory, Department of Bioengineering University of Pennsylvania, 240 Skirkanich Hall 210 S, 33rd St Philadelphia, PA 19104-6321, United States

ARTICLE INFO

Article history:
Accepted 19 March 2010

Keywords:
Collagen fiber
Injury biomechanics
Damage
Vector correlation
Ligament sprain

ABSTRACT

Many pathophysiological phenomena are associated with soft tissue loading that does not produce visible damage or tissue failure. As such, there is an unexplained disconnect between tissue injury and detectable structural damage during loading. This study investigated the collagen fiber kinematics of the rat facet capsular ligament to identify the onset of subfailure damage during tensile loading conditions that are known to induce pain. Quantitative polarized light imaging was used to determine the collagen fiber orientation in the capsular ligament ($n=7$) under tension, and an alignment vector correlation measurement was employed to identify local anomalous fiber realignment during loading. During the initial portion of loading when tissue stiffness was increasing, anomalous realignment was more likely to be detected than mechanical evidence of structural damage, and as a result, anomalous fiber realignment was identified significantly ($p=0.004$) before gross failure. The occurrence of anomalous fiber realignment was significantly associated ($p=0.013$) with a decrease in tangent stiffness during loading (ligament yield), suggesting this optical metric may be associated with a loss of structural integrity. The presence of localized anomalous realignment during subfailure loading in this tissue may explain the development of laxity, collagen fiber disorganization, and persistent pain previously reported for facet joint distractions comparable to that required for anomalous realignment. These optical data, together with the literature, suggest that mechanically induced tissue damage may occur in the absence of any macroscopic or mechanical evidence of failure and may produce local pathology and pain.

1. Introduction

Ligament sprains are among the most common injuries sustained during sports-related activities and motor vehicle crashes (Beynnon et al., 2005; Braun, 1999; Yawn et al., 2000). Significant advances have been made in biomechanical research to define and prevent gross ligament rupture, but less severe sprains also have the potential to lead to debilitating chronic conditions (Jones et al., 2009; Yang and King, 2003). For example, during rear-end automotive impacts, excessive facet capsular ligament stretch in the cervical spine has been hypothesized to lead to the symptoms of whiplash-associated disorders, among them long-lasting pain (Barnsley et al., 1994; Bogduk and Yoganandan, 2001; Lord et al., 1996; Stemper et al., 2005). While facet capsule strains, during simulations of these impacts, are significantly elevated over those during normal physiologic joint kinematics, the facet capsular ligament does not rupture (Deng et al., 2000; Panjabi et al., 1998; Pearson et al., 2004; Yoganandan et al., 1998). Yet, tissue rupture may not be a requisite for physiologic dysfunction after mechanical trauma. Biomechanical studies have identified collagen fiber disorganization, fibroblast necrosis, nociceptor activation, and persistent pain to result from ligament loading below the magnitudes needed to produce visible tissue rupture (Lee et al., 2004a; Lu et al., 2005b; Provenzano et al., 2002b; Quinn et al., 2007).

Several imaging techniques have been used in conjunction with mechanical testing to relate the structure and function of various soft tissues; but, few techniques have been used to identify injury without overt tissue rupture. Optical coherence tomography, small angle light scattering, and quantitative polarized light imaging have all been used to describe collagen fiber kinematics of soft tissue in response to various loading conditions (Billiar and Sacks, 1997; Hansen et al., 2002; Lake et al., 2009; Tower et al., 2002). Using quantitative polarized light imaging (QPLI), abnormal fiber kinematics were identified when both cadaveric and engineered tissue began to fail under tensile loading (Quinn and Winkelstein, 2008; Tower et al., 2002). Recently, correlations between fiber alignment vectors in sequential QPLI-derived alignment maps were measured to identify

* Corresponding author. Tel.: +1 215 573 4589; fax: +1 215 573 2071.
E-mail address: winkelst@seas.upenn.edu (B.A. Winkelstein).

0021-9290/$ - see front matter © 2010 Elsevier Ltd. All rights reserved.
doi:10.1016/j.jbiomech.2010.03.032

anomalous fiber realignment during loading in human cadaveric facet capsular ligament tissue (Quinn and Winkelstein, 2009). Specifically, the vector correlation between alignment maps was calculated on a pixel-by-pixel basis using both the fiber orientation and retardation (i.e. strength of alignment) from each of the surrounding pixels. Anomalous fiber realignment was identified by a decrease in the vector correlation in any group of connected pixels. This technique was based on the premise that when a collagen fiber breaks during loading, the local fiber network realigns as forces are redistributed to the remaining intact fibers. Detection of anomalous realignment coincided with a decrease in tangent stiffness or load during testing. The *initial* detection of anomalous realignment in that study was identified at significantly lower loads than for visible tissue damage. Although those findings suggested that anomalous collagen fiber kinematics may be related to microstructural damage before tissue rupture, the tissue tolerances that were defined by anomalous realignment for human tissue lacked physiological context, because they were derived from studies using cadaveric tissues.

The structural and physiological consequences of excessive capsular ligament stretch have been previously investigated using an in vivo rat model. Subfailure distractions of the rat cervical facet capsule to 0.7 mm produce persistent behavioral hypersensitivity mimicking pain (Lee et al., 2004b; Lee and Winkelstein, 2009). After the same subfailure in vivo loading paradigm, the standard deviation of collagen fiber directions was found to be significantly higher compared to uninjured rats in histological sections of the lateral aspect of the facet capsule (Quinn et al., 2007). Those findings suggest that the lateral aspect of the rat facet capsule may sustain microstructural damage during this painful subfailure loading condition. With such an established relationship between mechanical loading and the onset of persistent pain for the rat facet capsular ligament, the goal of the current study was to identify the onset of anomalous fiber realignment in the lateral facet capsule of the rat to determine the potential for localized microstructural damage at painful subfailure loading conditions. Because pathophysiological changes occur in this ligament following joint distractions of 0.7 mm, but not 0.2 mm (Lee et al., 2004b; Lee and Winkelstein, 2009), the initial detection of anomalous fiber realignment was hypothesized to also occur in that range. Given that the resolution of anomalous realignment detection can be easily adjusted by changing the image resolution, we also propose that in this smaller scale specimen, the optically based vector correlation technique may be more sensitive to initial microstructural damage than force-based metrics, in which accuracy depends on the signal-to-noise ratio of load measurements.

2. Methods

2.1. Specimen preparation

The C6/C7 motion segment was removed from Male Holtzman rats ($n=7$; 377 ± 12 g), and the left facet joint was carefully isolated and cleared of all musculature as previously described (Quinn et al., 2007; Quinn and Winkelstein, 2007). These methods were approved by our Institutional Animal Care and Use Committee. A custom-built interface with an Instron 5865 (Instron; Norwood, MA) applied tension across the C6/C7 facet joint by gripping each of the laminae and transverse processes of the C6 and C7 vertebrae with micro-forceps. The superior (C6) grips attached to a 10 N load cell (Instron; accuracy of 0.25% measured value).

The Instron was outfitted with a quantitative polarized light imaging system capable of acquiring pixel-wise collagen fiber alignment maps during continuous loading from the transmission of polarized light through the tissue, as previously described (Quinn and Winkelstein, 2008; Tower et al., 2002). To facilitate polarized light transmission through the rat facet capsule tissue only, articular bone was removed near the C6/C7 joint line. Specimens were positioned with the lateral aspect of the facet capsule facing the rotating polarizer (Fig. 1), and articular bone was removed from the secured specimens with a high-speed micro drill and a 0.7 mm diameter steel burr (Fine Science Tools; Foster City, CA).

2.2. Mechanical testing and data acquisition

After the articular bone was removed, the unloaded reference position of the specimen was set to have a distance of 2.53 mm between the midpoints of the C6 and C7 laminae, as in previous studies of this joint (Lee et al., 2008; Lee and Winkelstein, 2009; Quinn et al., 2007). Specimens were loaded in tension at a rate of 0.08 mm/s until complete rupture, with force and displacement data collected at 1 kHz. Fiber alignment maps were acquired with the QPLI system as described previously (Quinn and Winkelstein, 2008; Quinn and Winkelstein, 2009). In this study, imaging was performed using a Phantom-v9.1 camera (Vision Research; Wayne, NJ), at 200 Hz and a resolution of 40 pixels/mm. Light from a fiber-optic illuminator was transmitted through both a linear polarizer rotating at 300 rpm and the birefringent ligament tissue before entering a $6\times$ zoom lens outfitted with a circular analyzer (Fig. 1). Collagen fiber alignment maps were generated from every 20 images, corresponding to a full 180° rotation of the polarizer. As a result, alignment maps were produced at a rate of 10 Hz, which ensured that the tissue movement during loading would not exceed 0.32 pixels per alignment map. The intensity of light measured by the camera at each pixel was fit to a harmonic equation over every 20 frames. Based on the linear birefringence of the collagen fibers in the ligament tissue, the average fiber direction and retardation at each pixel were determined (Tower et al., 2002).

2.3. Detection of anomalous fiber realignment

The vector correlation of consecutive fiber alignment maps was used to detect anomalous fiber realignment. For every alignment map acquired, correlation measurements were made to identify changes in fiber realignment using the maps immediately preceding and following it. For each pixel, a vector correlation value was determined by comparing the data between alignment maps in a 5×5 pixel window centered at that pixel. This vector correlation measurement included both the mean fiber direction and the strength of alignment in that mean direction (i.e. retardation), and ranged from 0 to 1, with 1 being consistent alignment between maps (Quinn and Winkelstein, 2009). Vector correlation maps were produced for each fiber alignment map throughout the applied loading based on these pixel-by-pixel correlation calculations. The vector correlation was low in regions of the sample, where light transmission was poor due to obstruction by bone or synovial tissue. Pixels with an insufficient harmonic intensity response due to poor light transmission were identified through pixel-wise maps of the signal-to-noise ratio (SNR). Any pixels with an $SNR<2$ were removed from analysis due to a lack of consistent correlation values during the continuous acquisition of fiber data in static ligaments.

Anomalous collagen fiber realignment was defined by a decrease in the alignment vector correlation between maps. Specifically, anomalous realignment was defined at any pixel with an $SNR\geq2$, where the vector correlation decreased by 0.35 or more relative to its correlation value in the previous correlation map. This decrease in the vector correlation was selected based on a parametric analysis comparing the effect of the threshold value on the displacement at initial anomalous realignment detection. The displacement for initial detection showed little covariance with the threshold near a value of 0.35, and this threshold was also confirmed by the absence of any detection of anomalous realignment during data acquisition at 0 mm of displacement. Under the assumption that when a collagen fiber breaks, it causes anomalous realignment throughout the local fiber network, regions were defined as sustaining anomalous fiber realignment when at least nine pixels with anomalous realignment were connected to each other. The force and displacement at each alignment map, in which a region of anomalous fiber realignment was detected in the specimens, were recorded.

2.4. Mechanical data analysis

Gross failure, partial failure, and yield in each specimen were defined from the mechanical data to measure structural damage and provide context for the occurrence of anomalous fiber realignment. Prior to the analysis of failure or yield, force data were digitally filtered using a 10-point moving average with zero-phase distortion. Gross failure was defined by a drop in force after the maximum force during loading, and partial failure was defined by a decrease in force with increasing displacement between any two data points prior to gross failure. Ligament yield was defined by any decrease in the maximum tangent stiffness of at least 10% (Quinn and Winkelstein, 2008). By definition, for any data point where failure is detected, yield will also be detected because the tangent stiffness during failure decreases enough to become negative. For each specimen, all occurrences of yield or partial failure were identified during loading up to its gross failure.

2.5. Statistical analysis

The force and displacement at each of the initial detection of anomalous fiber realignment, yield, partial failure, and gross failure were compared through one-way ANOVAs with post-hoc Bonferroni tests. To determine whether anomalous

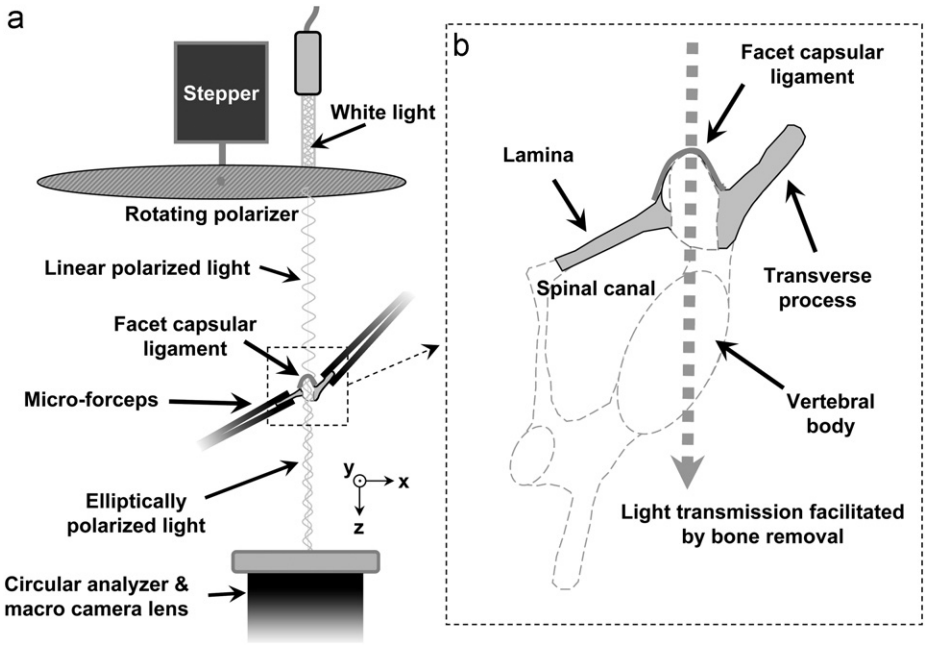

Fig. 1. Schematic representation of the QPLI setup and specimen from an overhead view. (a) Each specimen (in square) was mounted in the Instron with four micro-forceps attached to the laminae and transverse processes of C6 and C7. White light passed through a rotating polarizer, ligament tissue, and circular analyzer prior to image capture. Based on the polarizer orientation and collagen fiber birefringence, the average fiber orientation and strength of alignment were determined at each pixel. **(b)** To facilitate light transmission, the articular bone was removed between the camera and facet capsular ligament tissue; only the lamina and transverse process (dark gray regions) were left intact.

fiber realignment was significantly associated with the occurrence of yield and failure throughout loading, analysis was performed using a 2×2 contingency table. Data for the contingency table were calculated by partitioning the displacement data into sections based on whether or not yield or anomalous fiber realignment was detected from 0 mm to gross failure in each specimen. If neither were detected over a continuous section of displacement data, a single true-negative was counted in the contingency table. Likewise, if yield was detected over a period of displacement, and it coincided with the detection of realignment within that period, a single true-positive count was made. If either yield or realignment was solely detected over a section of the displacement, a count was made in one of the off-diagonal cells of the contingency table. Once the contingency table was assembled, each cell was checked to verify that its sample size was at least 10, and Pearson's Chi-square test analyzed the association between yield and anomalous fiber realignment. While the sensitivity of anomalous fiber realignment to yield depends on the proportion of the entire facet capsular ligament being analyzed during loading, the specificity to yield is unaffected by this factor. To provide context for this specificity value, the size (number of pixels) and occurrences (force and displacement) of anomalous realignment were compared between false- and true-positive detections for yield. The occurrences of these false- and true-positives were compared using an unpaired *t*-test; the size of anomalous realignment was compared between groups using a Wilcoxon rank-sum test due to the high deviations of the data from normality. Significance was defined by $\alpha = 0.05$ in all tests.

3. Results

Anomalous fiber realignment was detected in only 4.3% of all of the alignment maps generated during loading to gross failure for all specimens in this study. Realignment occurred across an average area of $0.033 \pm 0.049\ mm^2$ (53 ± 78 pixels) out of a total analyzed ligament area of $2.67 \pm 0.69\ mm^2$ (4273 ± 1105 pixels) (Fig. 2). Anomalous realignment was first detected at 0.62 ± 0.32 mm and 1.08 ± 0.79 N of loading (Tables 1 and 2). The initial detection of realignment was significantly correlated ($R = 0.903$, $p = 0.005$) with the initial detection of ligament yield (0.64 ± 0.24 mm, 1.12 ± 0.46 N). The first occurrence of failure occurred prior to reaching peak load in 6 of the 7 specimens (Tables 1 and 2), and this initial detection of failure was measured at 0.88 ± 0.18 mm and 2.03 ± 0.83 N. Gross failure occurred at a significantly greater displacement (1.14 ± 0.19 mm, $p = 0.004$) and force (2.69 ± 0.47 N, $p = 0.014$) than initial anomalous fiber realignment. Although the displacement at gross failure was significantly greater than at anomalous realignment, the displacements at these two events were significantly correlated (Table 1; $R = 0.769$, $p = 0.043$).

The detection of anomalous realignment and ligament yield were significantly associated ($p = 0.013$) through the contingency table analysis. The sensitivity of anomalous realignment to yield was 30.4%, and the specificity was 87.2%, leading to an overall accuracy of 63.4% for detecting yield through anomalous realignment. Although the detection of realignment was highly specific to yield during loading, the *initial* detection of realignment occurred in the absence of yield in 4 of the 7 specimens (Fig. 3; Table 1). Anomalous realignment without any detected yield or failure event (false-positive for yield) occurred at mean displacements (0.51 ± 0.17 mm) and forces (0.85 ± 0.48 N) that were significantly ($p < 0.001$) lower than realignment that coincided with a yield event (true-positive), occurring at 0.91 ± 0.20 mm and 1.99 ± 0.47 N. While anomalous fiber realignment without yield occurred earlier in the loading than realignment *with* yield, the average area of realignment was highly variable and not significantly different between events with (68 ± 92 pixels; $0.0426 \pm 0.0575\ mm^2$) and without (25 ± 26 pixels; $0.0156 \pm 0.0164\ mm^2$) yield.

4. Discussion

This study utilized vector correlation analysis to localize inferred microstructural damage during loading independent of mechanical data. Although calculated independently, anomalous fiber realignment was significantly associated with ligament yield ($p = 0.013$). Overall, anomalous fiber realignment was highly specific (87.2%) for the occurrence of yield, but when anomalous realignment did occur without yield detection, it took place at significantly lower ($p < 0.001$) magnitudes of loading than realignment *with* yield. This finding suggests that at lower

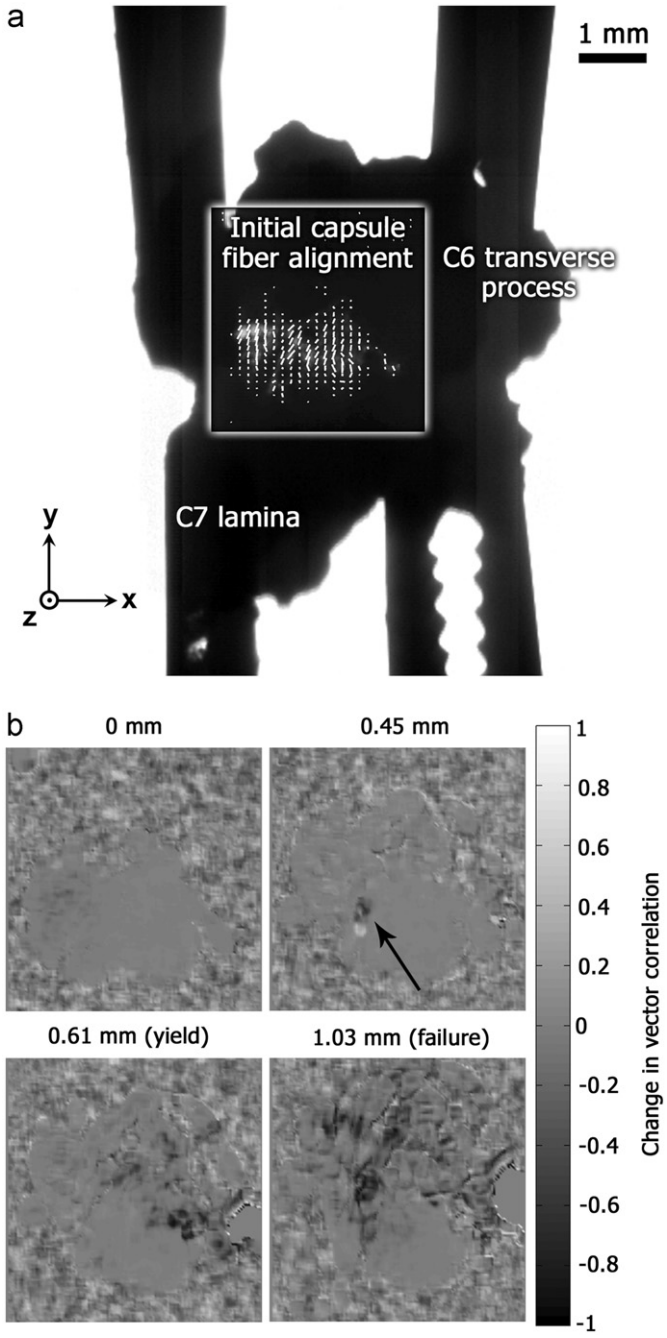

Fig. 2. Detection of anomalous fiber realignment in specimen AZ. (a) The initial collagen fiber alignment with fiber alignment vectors plotted every five pixels shows the tissue region with sufficient signal-to-noise before loading. **(b)** Anomalous fiber realignment, defined by a significant negative change in vector correlation values, was first observed at 0.45 mm of displacement (indicated by arrow), but was also detected during the onset of yield and gross failure.

magnitudes of loading, the optical detection of anomalous realignment could, in fact, be more sensitive than yield to microstructural damage. Yield may be particularly insensitive to damage during the initial portion of tissue loading, because decreases in stiffness due to the breaking of fibers could be offset by the increasing stiffness of the tissue as other collagen fibers are becoming engaged. Although previous use of this vector correlation technique with human tissue did not identify any anomalous realignment without ligament yield (Quinn and Winkelstein, 2009), the sensitivity of anomalous realignment detection was enhanced in the current study by the 10-fold increase in spatial resolution due to a higher lens magnification used for these smaller specimens.

Table 1
Displacement (mm) at the initial detection of gross failure, partial failure, yield, and anomalous realignment.

Specimen	Gross failure	Partial failure	Yield	Anomalous realignment
AZ	1.03	0.62	0.61	0.45[a]
N3	1.07	0.96	0.63	0.84
N4	0.93	0.93[†]	0.26	0.20[a]
N5	1.16	0.99	0.55	0.49[a]
N6	1.50	0.93	0.91	0.91
N7	1.02	0.63	0.57	0.36[a]
N8	1.28	1.07	0.97	1.07
Mean	**1.14**	**0.88**	**0.64**	**0.62**
SD	**0.19**	**0.18**	**0.24**	**0.32**
Correlation	0.769*	0.556	0.903*	

[†] The first detected failure event was at gross failure.
[a] Anomalous realignment was detected without yield.
* The correlation of each of the mechanical metrics with initial anomalous realignment was calculated, with significant values indicated.

Table 2
Force (N) at the initial detection of gross failure, partial failure, yield, and anomalous realignment.

Specimen	Gross failure	Partial failure	Yield	Anomalous realignment
AZ	2.41	0.92	0.90	0.37[a]
N3	2.39	2.08	1.01	1.69
N4	3.54	3.54[†]	0.75	0.60[a]
N5	2.36	2.27	0.55	0.45[a]
N6	3.14	1.84	1.77	1.75
N7	2.30	1.34	1.15	0.48[a]
N8	2.70	2.25	1.68	2.25
Mean	**2.69**	**2.03**	**1.12**	**1.08**
SD	**0.47**	**0.83**	**0.46**	**0.79**
Correlation	0.165	0.126	0.790*	

[†] The first detected failure event was at gross failure.
[a] Anomalous realignment was detected without yield.
* The correlation of the forces from each of the mechanical metrics with initial anomalous realignment was calculated, with significant values indicated.

These findings suggest that a vector correlation technique may be capable of localizing microstructural damage at the pixel-level, but there is an inherent difficulty in validating a methodology to identify a previously undetectable class of injuries. In lieu of actually visualizing when a collagen fiber breaks during loading, this study measured the local fiber kinematic response and examined the relationship between mechanics and anomalous realignment to evaluate the potential for microstructural damage during anomalous realignment. Although a significant relationship was found between mechanical evidence of damage (i.e. yield) and anomalous realignment (Tables 1 and 2), additional histological or ultrastructural studies would confirm the presence of structural damage at the initial detection of anomalous realignment. Yet, such evaluations are difficult due to variability in the initial onset of anomalous realignment (Table 1), and would require a real-time assessment of vector correlation. As a result, it remains unknown whether the cause of anomalous realignment is always due to a collagen fiber or crosslink breaking under tension, or whether detection can also be the byproduct of other phenomena, such as the rapid untangling of two or more fibers.

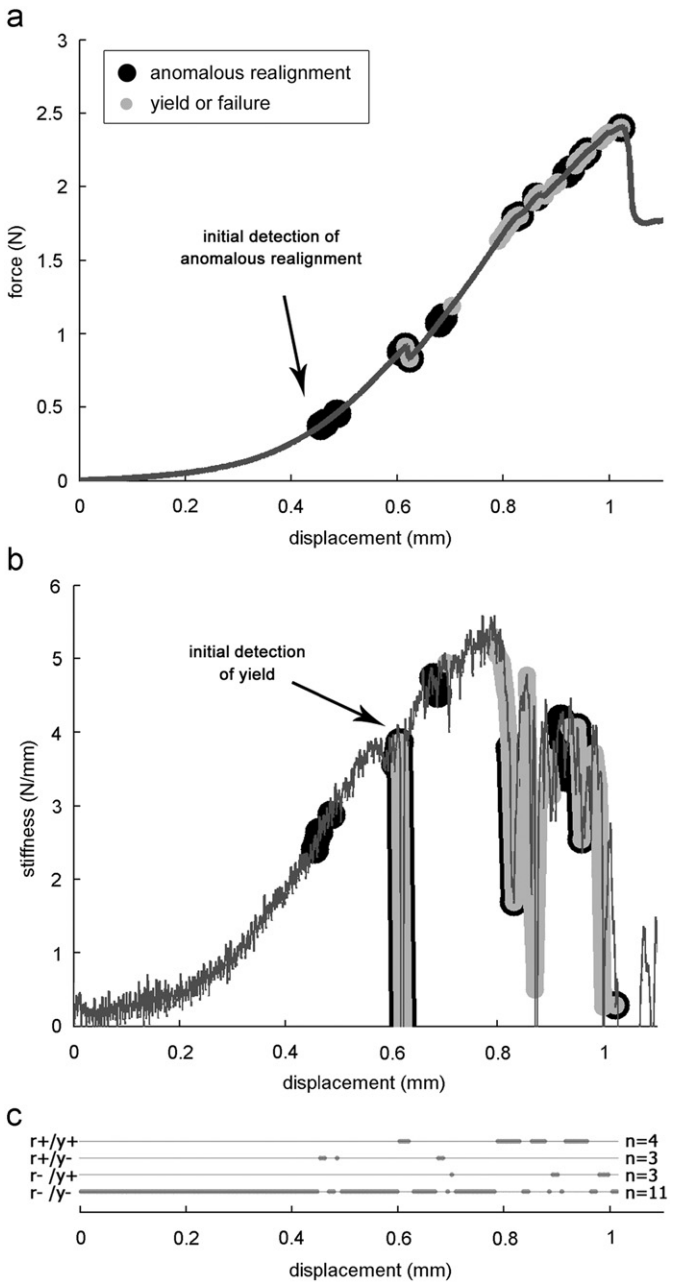

Fig. 3. Mechanical data from a representative specimen (AZ). (a) Anomalous fiber realignment was first detected at 0.45 mm of displacement with no measurable decrease in force or stiffness. **(b)** The first occurrence of yield was detected at 0.61 mm. **(c)** Displacement data were partitioned into sections for contingency table analysis based on whether realignment (r) and/or yield (y) was detected. The detection of realignment and yield coincided four times prior to gross failure of this specimen. Realignment detection without yield ($n=3$) was more likely to occur earlier during loading than the detection of yield without realignment ($n=3$).

The low sensitivity of anomalous realignment to yield (30.4%) also highlights a limitation of this optical technique in that detection can only occur within the portion of the tissue being imaged. Because the capsular ligament in the rat covers the facet joint from the lamina to the transverse process (Fig. 1), only a portion of the capsule was imaged in this study. Thus, any microstructural damage that may have occurred in the other dorsal–medial and ventral–lateral regions of the capsular ligament would have been missed by the vector correlation technique. This limitation in the camera field of view may contribute to the low sensitivity of realignment to yield, and would suggest that the average structural threshold for anomalous realignment in the entire capsular ligament may be lower than 0.63 ± 0.32 mm (Table 1). Nonetheless, within the portion of the lateral capsule that was imaged, anomalous realignment may provide the most accurate detection of microstructural damage given that it can be assessed on a pixel-by-pixel basis rather than from the overall mechanical response of the tissue.

This is the first optical evidence suggestive of microstructural damage in the lateral facet capsule during loading within the range of joint displacements corresponding to the induction of persistent pain in the rat. The current study detected anomalous realignment in that aspect of the joint at displacements (0.62 ± 0.32 mm; Table 1) near the 0.7 mm that produces collagen fiber disorganization in the lateral capsule, increased expression of pain-related neuromodulators in the peripheral and central nervous system, and significant behavioral hypersensitivity (Lee and Winkelstein, 2009; Quinn et al., 2007). Electrophysiological studies have also provided evidence of facet-mediated pain through the identification of nociceptor activation and mechanoreceptor saturation at loading magnitudes below gross tissue rupture (Lu et al., 2005a; Lu et al., 2005b). However, in all of those studies, the threshold for subfailure injury was inferred using peak strain in the facet capsule due to a lack of any visual evidence of damage. The optical technique in the current study provides a method to identify rapid changes in the fiber realignment patterns of the tissue's collagen matrix during loading (Fig. 2), and suggests that an anomalous change in fiber organization may be sufficient to initiate physiological changes and sensitize local nociceptors and mechanoreceptors in the facet joint.

Structural damage from subfailure loading has been inferred primarily through changes in the mechanical responses of soft tissue. Previous work has demonstrated unrecoverable laxity following loading that produces low-grade ligament sprains (Panjabi et al., 1996; Provenzano et al., 2002a; Provenzano et al., 2002b; Quinn et al., 2007). Additionally, decreased tissue stiffness and altered viscoelastic properties have been identified (Panjabi and Courtney, 2001; Panjabi et al., 1999), but no study has been able to identify a specific point *during* loading when the tissue structure changes during assumed injurious loading. In addition to the potential for generating pain (Cavanaugh et al., 2006; Lee et al., 2004b; Lee and Winkelstein, 2009; Lu et al., 2005a; Lu et al., 2005b), subfailure loading produces an increase in fibroblast-mediated remodeling (Provenzano et al., 2005), further suggesting the occurrence of structural damage prior to tissue failure. These studies attributed an array of mechanical and cellular responses to tissue damage from subfailure loading, but required multiple specimens to identify an injury threshold. However, the current study provides a method to determine the onset of microstructural damage for individual specimens.

This study demonstrates that the fiber kinematics within a capsular ligament significantly deviate from their normal realignment patterns before gross tissue failure occurs. Anomalous collagen fiber realignment can occur without visible changes, obvious on the tissue's surface. Yet, the initial detection of realignment is strongly correlated with a loss of tissue stiffness, resulting in the detection of ligament yield (Tables 1 and 2). As such, these findings begin to provide an explanation for the host of structural and physiological changes that can occur in soft tissue following excessive loading without overt tissue rupture. By identifying a fiber phenomenon that would seem to indicate damage during subfailure loading, this technique describes a direct method to define the loading magnitudes that produce moderate ligament sprains, and may provide a means to compare mechanical tolerances for pathological changes across different tissues and species without needing complex scaling algorithms.

Conflict of interest

There are no conflicts of interest for any authors with any aspect of this study.

Acknowledgments

This material is based on work supported by the National Science Foundation under Grant no. 0547451, and was also funded by support from the Catharine D. Sharpe Foundation and the Defense University Research Instrumentation Program of the U.S. Army Research Office.

References

Barnsley, L., Lord, S., Bogduk, N., 1994. Whiplash injury. Pain 58, 283–307.
Beynnon, B.D., Vacek, P.M., Murphy, D., Alosa, D., Paller, D., 2005. First-time inversion ankle ligament trauma: the effects of sex, level of competition, and sport on the incidence of injury. American Journal of Sports Medicine 33, 1485–1491.
Billiar, K.L., Sacks, M.S., 1997. A method to quantify the fiber kinematics of planar tissues under biaxial stretch. Journal of Biomechanics 30, 753–756.
Bogduk, N., Yoganandan, N., 2001. Biomechanics of the cervical spine Part 3: minor injuries. Clinical Biomechanics 16, 267–275.
Braun, B.L., 1999. Effects of ankle sprain in a general clinic population 6 to 18 months after medical evaluation. Archives of Family Medicine 8, 143–148.
Cavanaugh, J.M., Lu, Y., Chen, C., Kallakuri, S., 2006. Pain generation in lumbar and cervical facet joints. Journal of Bone and Joint Surgery—American 88, 63–67.
Deng, B., Begeman, P.C., Yang, K.H., Tashman, S., King, A.I., 2000. Kinematics of human cadaver cervical spine during low speed rear-end impacts. Stapp Car Crash Journal 44, 171–188.
Hansen, K.A., Weiss, J.A., Barton, J.K., 2002. Recruitment of tendon crimp with applied tensile strain. Journal of Biomechanical Engineering 124, 72–77.
Jones, L., Bismil, Q., Alyas, F., Connell, D., Bell, J., 2009. Persistent symptoms following non operative management in low grade MCL injury of the knee—the role of the deep MCL. Knee 16, 64–68.
Lake, S.P., Miller, K.S., Elliott, D.M., Soslowsky, L.J., 2009. Effect of fiber distribution and realignment on the nonlinear and inhomogeneous mechanical properties of human supraspinatus tendon under longitudinal tensile loading. Journal of Orthopaedic Research 27, 1596–1602.
Lee, K.E., Davis, M.B., Mejilla, R.M., Winkelstein, B.A., 2004a. In vivo cervical facet capsule distraction: mechanical implications for whiplash and neck pain. Stapp Car Crash Journal 48, 373–395.
Lee, K.E., Davis, M.B., Winkelstein, B.A., 2008. Capsular ligament involvement in the development of mechanical hyperalgesia after facet joint loading: behavioral and inflammatory outcomes in a rodent model of pain. Journal of Neurotrauma 25, 1383–1393.
Lee, K.E., Thinnes, J.H., Gokhin, D.S., Winkelstein, B.A., 2004b. A novel rodent neck pain model of facet-mediated behavioral hypersensitivity: implications for persistent pain and whiplash injury. Journal of Neuroscience Methods 137, 151–159.
Lee, K.E., Winkelstein, B.A., 2009. Joint distraction magnitude is associated with different behavioral outcomes and substance P levels for cervical facet joint loading in the rat. Journal of Pain 10, 436–445.
Lord, S.M., Barnsley, L., Wallis, B.J., Bogduk, N., 1996. Chronic cervical zygapophysial joint pain after whiplash. A placebo-controlled prevalence study. Spine 21, 1737–1745.
Lu, Y., Chen, C., Kallakuri, S., Patwardhan, A., Cavanaugh, J.M., 2005a. Neural response of cervical facet joint capsule to stretch: a study of whiplash pain mechanism. Stapp Car Crash Journal 49, 49–65.
Lu, Y., Chen, C., Kallakuri, S., Patwardhan, A., Cavanaugh, J.M., 2005b. Neurophysiological and biomechanical characterization of goat cervical facet joint capsules. Journal of Orthopaedic Research 23, 779–787.
Panjabi, M.M., Cholewicki, J., Nibu, K., Grauer, J., Vahldiek, M., 1998. Capsular ligament stretches during in vitro whiplash simulations. Journal of Spinal Disorders and Techniques 11, 227–232.
Panjabi, M.M., Courtney, T.W., 2001. High-speed subfailure stretch of rabbit anterior cruciate ligament: changes in elastic, failure and viscoelastic characteristics. Clinical Biomechanics 16, 334–340.
Panjabi, M.M., Moy, P., Oxland, T.R., Cholewicki, J., 1999. Subfailure injury affects the relaxation behavior of rabbit ACL. Clinical Biomechanics 14, 24–31.
Panjabi, M.M., Yoldas, E., Oxland, T.R., Crisco 3rd, J.J., 1996. Subfailure injury of the rabbit anterior cruciate ligament. Journal of Orthopaedic Research 14, 216–222.
Pearson, A.M., Ivancic, P.C., Ito, S., Panjabi, M.M., 2004. Facet joint kinematics and injury mechanisms during simulated whiplash. Spine 29, 390–397.
Provenzano, P.P., Alejandro-Osorio, A.L., Valhmu, W.B., Jensen, K.T., Vanderby Jr., R., 2005. Intrinsic fibroblast-mediated remodeling of damaged collagenous matrices in vivo. Matrix Biology 23, 543–555.
Provenzano, P.P., Hayashi, K., Kunz, D.N., Markel, M.D., Vanderby Jr., R., 2002a. Healing of subfailure ligament injury: comparison between immature and mature ligaments in a rat model. Journal of Orthopaedic Research 20, 975–983.
Provenzano, P.P., Heisey, D., Hayashi, K., Lakes, R., Vanderby Jr., R., 2002b. Subfailure damage in ligament: a structural and cellular evaluation. Journal of Applied Physiology 92, 362–371.
Quinn, K.P., Lee, K.E., Ahaghotu, C.C., Winkelstein, B.A., 2007. Structural changes in the cervical facet capsular ligament: potential contributions to pain following subfailure loading. Stapp Car Crash Journal 51, 169–187.
Quinn, K.P., Winkelstein, B.A., 2007. Cervical facet capsular ligament yield defines the threshold for injury and persistent joint-mediated neck pain. Journal of Biomechanics 40, 2299–2306.
Quinn, K.P., Winkelstein, B.A., 2008. Altered collagen fiber kinematics define the onset of localized ligament damage during loading. Journal of Applied Physiology 105, 1881–1888.
Quinn, K.P., Winkelstein, B.A., 2009. Vector correlation technique for pixel-wise detection of collagen fiber realignment during injurious tensile loading. Journal of Biomedical Optics 14, 054010.
Stemper, B.D., Yoganandan, N., Pintar, F.A., 2005. Effects of abnormal posture on capsular ligament elongations in a computational model subjected to whiplash loading. Journal of Biomechanics 38, 1313–1323.
Tower, T.T., Neidert, M.R., Tranquillo, R.T., 2002. Fiber alignment imaging during mechanical testing of soft tissues. Annals of Biomedical Engineering 30, 1221–1233.
Yang, K.H., King, A.I., 2003. Neck kinematics in rear-end impacts. Pain Research and Management 8, 79–85.
Yawn, B.P., Amadio, P., Harmsen, W.S., Hill, J., Ilstrup, D., Gabriel, S., 2000. Isolated acute knee injuries in the general population. The Journal of Trauma 48, 716–723.
Yoganandan, N., Pintar, F.A., Klienberger, M., 1998. Cervical spine vertebral and facet joint kinematics under whiplash. Journal of Biomechanical Engineering 120, 305–307.